Indian Journal of Pure & Applied Physics
Vol. 61, July 2023, pp. 541-545
DOI: 10.56042/ijpap.v61i7.102

Nonlinear Optical Absorption Properties of Sputtered WSe_2 Thin-films in the Near-Infrared Spectral Band

Km. Surbhi & Ritwick Das*

School of Physical Sciences, National Institute of Science Education and Research, An OCC of Homi Bhabha National Institute, Jatni, Odisha – 752 050, India

Received 16 October 2022; accepted 12 June 2023

We present a detailed investigation on the intensity dependent third-order nonlinear optical (NLO) properties of RF-sputtered WSe_2 thin film using ultra short pulses. The investigation employed a single-beam Z-scan technique using near-infrared (NIR) ultra short pulses centered at 1030 nm for ascertaining the NLO response. The results reveal a reverse saturable absorption (RSA) signature, which is primarily due to the contribution from two-photon absorption (TPA). We explored the impact of high optical fluence on the TPA process and observed the weakening of the nonlinear optical absorption in WSe_2 thin film, which essentially pointed towards a significant contribution of free-carriers as well as band-filling effect. This research elucidates the insight of photophysical properties of WSe_2 thin films and shows the potential use as optical limiters.

Keywords: WSe_2 Thin films; Nonlinear optical process; Two-photon absorption; Free-charge carriers, Transition-metal dichalcogenides

1 Introduction

Passive optical power limiters have been widely employed in optical communications and military applications such as to provide frequency-agile protection by limiting the influx of hazardous radiation. The potential advantage is derived from the possibility of inherent and automated control due to the fact that the optical limiting properties originate from the intrinsic properties of the material. From an application viewpoint, the third order optical nonlinearity which includes the nonlinear absorption (NLA) is becoming a crucial physical quantity to ascertain and analyze. In addition, the materials exhibiting high optical nonlinearity induced absorption have found applications in a wider spectrum including optical switch designing, optical routing in monolithically integrated optical circuitry and optical channel blocking as well as limiting. From a material perspective, two-dimensional (2D) sub-wavelength materials are an emergent and promising platform for photonic and opto-electronic applications. The discovery of graphene has opened up a door to a novel world of 2D-layered materials. The limitations of graphene for a broad range of applications have pivoted the exploration of a wider class of 2D materials known as transition metal dichalcogenides (TMDs). TMDs, by virtue of facilitating strong spin-orbit coupling, exhibit unique and versatile physical, chemical and thermal properties which have a discernible thickness-dependence. Such a feature is essentially brought about by strong intra-layer covalent bond and weak inter-layer vander Waals forces which also permits TMDs to be fabricated into compact, efficient and flexible optical devices. It is worth pointing out that the variation in optical properties of TMD thin-films are governed by the alteration in the electronic band structure of the TMD thin-films which, itself, is a function of the number of monolayers stacked together[1–3]. From the perspective of nonlinear optics, such thickness dependent variation in electronic bandgap is very attractive owing to the fact that this modifies the hyperpolarizability in material species. The deployment of TMDs for photonic applications such as optical limiting[4], Q-switching[5], mode-locking[6], and optical switching[7] has produced devices with high performance and unique functions. In addition, the impact of high optical fluence on the TMD films is extremely crucial from the application point of view. At high optical intensities, TMDs thin films are expected to exhibit free-charge carrier induced modifications in electron transport properties

*Corresponding author: (E-mail: ritwick.das@niser.ac.in)

which could affect the device performance during operation. Therefore, the possible modifications in the NLO behaviour of TMD films at high optical intensities in the desirable spectral band require further investigation. In this work, we present a detailed investigation of nonlinear optical properties of WSe_2 thin film using single-beam Z-scan technique. The study reveals that the nonlinear absorption in RF-sputtered WSe_2 thin-film exhibits reverse saturable absorption behaviour at 1030 nm excitation wavelength. However, there is a gradual weakening in the absorption at higher optical intensities which could essentially be attributed to free-carrier absorption.

2 Experimental Details

2.1 Sample preparation

WSe_2 thin-films of a desired thickness were prepared onto a 1 × 1 cm^2 glass substrate using a RF magnetron sputtering system with a WSe_2 (99.9% pure) target in an argon environment at room temperature. Before the deposition, the chamber was evacuated by turbo- molecular pump to a vacuum of 3.1×10^{-6} mbar. Throughout the deposition process, the Ar gas concentration was maintained at 15 sccm, and the power was fixed at 60 W. The deposition was performed at a pressure of 1×10^{-2} mbar. The morphological study of the RF-sputtered WSe_2 thin-film is done through field-emission scanning electron microscope (FESEM). The Raman spectrum was carried out using a Raman spectrometer (Jobin Yvon Lab Ram HR Evolution, Horiba) with an excitation at 532 nm wavelength. The linear absorption spectrum of the WSe_2 thin film was measured using a UV-VIS-NIR spectrometer (Agilent cary 5000 UV-Vis-NIR).

2.2 Z-scan experimental set up

The nonlinear optical absorption measurements of WSe_2 thin-film was carried out through single-beam Z-scan technique which used a Fourier-transform limited (FTL) ultrashort pulses of temporal width of ≈ 370 fs at 1030 nm excitation wavelength. The pulse repetition rate was chosen to be 100 kHz. The optical power of the incident beam is controlled by a combination of half waveplate (HWP) and a polarizing beam-splitter (PBS). The laser beam is focused to a suitable spot-size of ≈ 30 μm using a thin plano-convex lens of focal length 100 mm. This results in a Rayleigh length of 2.39 mm which is significantly greater than the WSe_2 film thickness. The WSe_2 thin film was translated by ≈ 10 cm symmetrically about the focal point. The optical nonlinearities in the films manifested when the incident intensity of the focused laser beam was intense enough and the transmittance modified as the film was translated through the focal plane. In order to perform the open-aperture (OA) Z-scan measurement the aperture was kept open and the transmitted laser beam through the sample was collected on to the detector.

3 Results and Discussion

The homogeneity of the structure and the thickness of the sample is estimated from field-emission scanning electron microscope (FESEM). The cross-sectional FESEM is performed to obtain the thickness of the deposited thin film. In Fig. 1(a), the representative top-view image of WSe_2 thin film is shown. The image shows acceptable homogeneity and continuity in WSe_2 films. The inset shows the cross-sectional image and the measured thickness is ≈ 30 nm. Raman spectroscopy was employed to ascertain the vibrational modes of the deposited thin WSe_2 film. Fig. 1(b) represents the Raman spectrum for the WSe_2 thin-film which depicts the three characteristic phonon modes. The peak corresponding

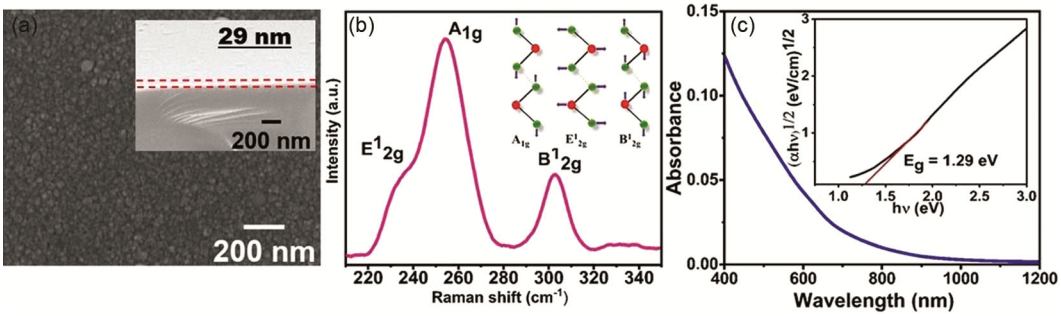

Fig. 1 — (a) Shows the top surface image of WSe_2 thin film obtained using a Field Emission Scanning Microscope (FESEM). Inset: shows cross-sectional FESEM image for determining film thickness (29 nm). (b) Raman spectrum of WSe_2 thin film. (c) Absorption spectrum for WSe_2 thin film in the visible and near-infrared spectral band. Inset: shows the Tauc plot for estimating the indirect bandgap of WSe_2 film.

to E^1_{2g} mode is associated with in-plane vibration of W and Se atoms. The sharp peak corresponding to A_{1g} is related to out-of-plane vibration of Se atoms. The peak corresponding to B^1_{2g} mode is essentially due to the vibration of W and Se atoms owing to the interlayer interactions[8]. In order to give a clear insight, the schematic representation of vibrational modes is given in inset. The linear absorption spectrum for the WSe_2 thin film is measured using UV-visible spectroscopy which is shown in Fig. 1(c). The absorbance reduces at longer wavelengths and turns negligible for wavelengths above 1000 nm. The estimation of indirect bandgap is obtained from the Tauc fitting expression given by[8],

$$\alpha h\nu = A(h\nu - E_g)^n \quad \ldots (1)$$

where α, hν, A and E_g are the linear absorption coefficient, photon energy, a constant and the bandgap respectively, we obtain the indirect bandgap of WSe_2 film by extrapolating the linear part of the plot between $(\alpha h\nu)^{1/2}$ and hν (see inset of Fig.1(c)). The estimated value of indirect bandgap is 1.29 eV which is close to that for bulk WSe_2 crystal. The nonlinear optical properties of WSe_2 thin film was investigated using single-beam OA Z-scan technique which yields the nonlinear optical absorption coefficient β. As mentioned before, the excitation source (pump laser) emits 370 fs pulses centered at 1030 nm at a repetition rate of 1 kHz. It is important to point out that the excitation photon energy is lesser than the intrinsic bandgap of the WSe_2 film. Figure 2 shows the measured OA normalized transmission (dotted curve) for the WSe_2 thin-film at a fixed on-axis peak laser intensity I_0 = 3.29 GW/cm^2 at the focal plane. The transmittance curve is characterized by a transmission minima at the focal plane *i.e.* z = 0 which is a signature of reverse saturable absorption (RSA). This essentially implies that the RSA signature is a consequence of a two-photon absorption (TPA) which is expected for a 1030 nm excitation wavelength.

In order to quantitatively estimate β, the measured OA normalized transmittance were fitted using the expression[9]

$$\Delta T = 1 - \frac{\beta_{eff} I_0 L_{eff}}{2^{3/2}(1+x^2)} \quad \ldots (2)$$

where β_{eff} is the nonlinear absorption coefficient, I_0 is the intensity of laser beam at focal plane (*i.e.* z = 0), $L_{eff} = (1 - e^{-\alpha L})/\alpha$, L is the length of sample, α is linear absorption coefficient, $x = z/z_0$, z is the sample position and $z_0 = \pi\omega_0^2/\lambda$ is defined as the Rayleigh length of the pump laser beam.

The imaginary part of the complex third order nonlinear susceptibility ($\chi^{(3)}_{Im}$) was obtained from β using the relation[10]

$$\chi^{(3)}_{Im} = \left[\frac{10^{-7} c n^2 \lambda}{96\pi^2}\right]\beta \quad \ldots (3)$$

where c is the speed of light in vacuum, n is the linear index of refraction and λ is the excitation wavelength of the laser beam. In order to eliminate the overestimation in β brought about by linear absorption α, we define a figure of merit (FOM) as FOM = $|\chi^{(3)}_{Im}/\alpha|$ which provides a relative estimate of β with respect to the linear absorption. In Table 1, the values of β and FOM has been tabulated for different intensities. It could be observed that the linear transmittance and linear absorption of the film are 76.11% and 3.37 × 10^4 cm^{-1} respectively. The value of β corresponding to Fig. 2 is 250.1×10^{-7} cm/W and FOM is 70.12×10^{-14} esu.cm.

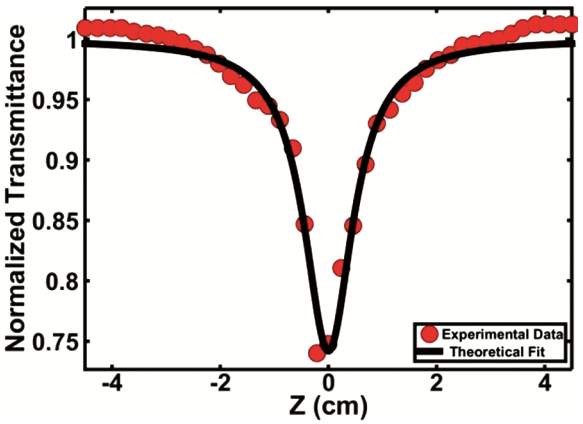

Fig. 2 — Variation of normalized transmission through WSe_2 thin-film as a function of translation distance (z) for an on-axis peak laser intensity of I_0 = 3.29 GW/cm^2 (dotted-red curve) in open-aperture Z-scan measurement. The black-solid lines are theoretical fitting to the experimental measurement using Eq. (2).

Table 1 — Estimated values of TPA coefficient, imaginary part of χ(3) and figure of merit (FOM) for the WSe_2 thin film.

Sample (nm)	T_0(%)	α ×10^4 (cm^{-1})	I_0 × 10^9 (W/cm^2)	β × 10^{-7} (cm/W)	Im[$\chi^{(3)}$] × 10^{-9} (esu)	FOM×10^{-14}(esu cm)
29	76.11	3.37	3.29	250.1	23.63	70.12
			12.76	61.50	5.99	17.78
			66.85	12.39	2.16	6.41
			217.73	3.168	1.12	3.32
			407.45	1.46	0.39	1.16

In general, the thin film architectures are characterized by grain boundaries and associated defects which could have an impact on the electronic band structure. This could affect the optical absorption process that could manifest through the generation of 'free-carriers'. Consequently, the hyperpolarizability and measure of NLO coefficients may exhibit characteristics which depend on laser power, repetition rate and pulse width or overall the pump laser intensity. Therefore, it is worth investigating the impact of optical intensity on the NLO properties of WSe_2 thin film. In order to investigate the role of laser intensity, we observed the variation in the estimated values of β of the WSe_2 thin film as a function of on-axis peak intensity at focal plane (*i.e.* I_0) which is presented in Fig. 3. It is apparent that the WSe_2 thin film exhibits maximum β at the small laser intensity and drops sharply for $I_0 \gtrsim 5$ GW/cm^2. Further, the variation in β monotonically decreases at higher laser powers which could also be observed in Table 1. This signature in the TPA variation depicts a discernible contribution from 'free-charge carriers' in the nonlinear absorption process[11]. In other words, we note that the bottom of the conduction band has a high population density at high laser intensities owing to appreciable TPA led transitions. A nominal rise in intensity thereafter could drive the system into saturation. The excess 'free' charge carriers in the conduction band could further contribute to linear absorption through excitation to higher energy bands. This is known as 'free' carrier induced absorption. However, the nonlinear absorption process would weaken, in that case which would result in a smaller β. This reduction in β is lead by TPA-induced FCA and have been investigated previously in semiconducting thin-film based configurations[12-14].

In addition to the free-carrier led nonlinear absorption, the thickness dependent bandgap in WSe_2 thin films play a pivotal role in tailoring the TPA behaviour in WSe_2 films. This has been explored in detail and reported elsewhere[8]. In order to present a comparative insight, we have tabulated the values of *β* in Table 2 for a few TMD based films using different excitation sources. It is apparent that all the measurements yield TPA behavior at near-infrared wavelengths (1040 nm and 1064 nm). It is worthwhile to note that the TPA coefficient for the WSe_2 film is at least an order of magnitude greater than the reported values TMDs such as WS_2, MoS_2, $MoSe_2$ and $Mo_{0.5}W_{0.5}S_2$.

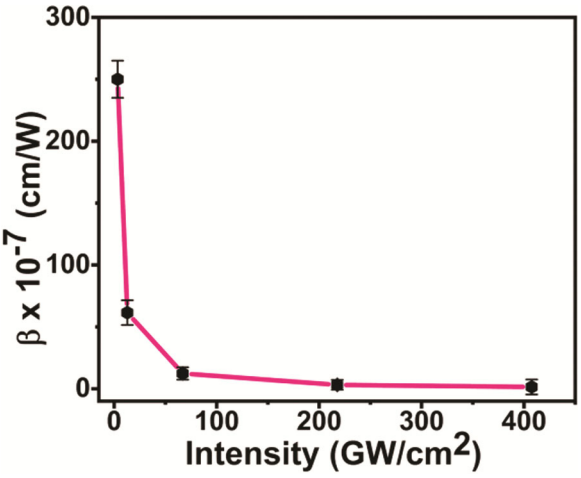

Fig. 3 — Variation of TPA coefficient β as a function of on-axis peak laser intensity at the focal plane (I_0).

Table 2 — A comparison depicting the values of β (RSA behavior) for transition metal dichalcogenides using various excitation sources.

Sample	β(cm/W)	Wavelength and pulse width	References
WSe_2	7.29×10^{-6}	1064 nm, 25 ps	[6]
$W_{0.5}Mo_{0.5}$ Se_2	1.9×10^{-9}	1064 nm, 25 ps	[15]
$W_{0.5}S_2$	1.91 x10^{-8}		
WS_2	1.81×10^{-6}	1040 nm, 340 fs	[16]
WSe_2	2.14×10^{-6}		
MoS_2–H	8.0×10^{-14}	1030 nm, 340 fs	[17]
$MoSe_2$–H	2.0×10^{-13}		
MoS_2	5.0×10^{-10}	532 nm, 19 ps	[18]
WS_2	1.2×10^{-9}		
MoS_2	66.0×10^{-9}	1030 nm, 340 fs	[10]
WS_2	12.75×10^{-6}		
WSe_2	2.5×10^{-5}	1030 nm, 370 fs	This work

4 Conclusions

In conclusion, we have investigated the nonlinear optical absorption process in WSe_2 thin-films using single-beam Z-scan technique which involved ultrashort pulses centered at 1030 nm. We found that WSe_2 thin film exhibit RSA behavior which is a consequence of TPA. It is interesting to note that the TPA process generates additional free-charge carriers in the film at high laser intensities which, in turn reduce the TPA coefficient. Elsewhere reported nonlinear refractive indices and the TPA coefficients of WSe_2 thin films indicate their potential for application in communication technology[19]. The variation in the nonlinear absorption exhibited by the film points toward the possibility of bandgap engineering led improvement in functionality of semiconducting thin-film based photonic limiters, sensors and data-storage configurations.

Acknowledgement

We thank the National Institute of Science Education and Research, Department of Atomic Energy (DAE), In-dia for the funding to carry out this work.

References

1 Yun W S, Han S W, Hong S C, Kim I G & Lee J D, *Phys Rev B*, 85 (2012) 033305.
2 Zhao W, Ghorannevis Z, Chu L, Toh M, Kloc C, Tan P H & Eda G, *ACS Nano*, 7 (2013) 791.
3 Pandey S K, Das R & Mahadevan P, *ACS Omega*, 5 (2020) 15169.
4 Loh K P, Zhang H, Chen W Z & Ji W, *The J Phys Chem B*, 110 (2006) 1235.
5 Chen B, Zhang X, Wu K, Wang H, Wang J & Chen J, *Opt Exp*, 23 (2015) 26723.
6 Liu W, Liu M, Ou Y Y, Hou H, Ma G, Lei M & Wei Z, *Nanotechnology*, 29 (2018) 174002.
7 Boyd R W, Nonlinear Optics, Academic Press, (2020).
8 Surbhi K, Bhakta S, Kumari A, Sahoo U P, Sahoo P K & Das R, *Opt Mater*, 129 (2022) 112479.
9 Sheik-Bahae M, Said A A, Wei T H, Hagan D J & Van Stryland E W, *IEEE J Quant Electron*, 26 (1990) 760.
10 Zhang S, Dong N, McEvoy N, O'Brien M, Winters S, Berner N C & Wang J, *ACS Nano*, 9 (2015) 7142.
11 James R & Smith D, *IEEE J Quant Electr*, 18 (1982) 1841.
12 Surbhi K, Bhakta S, Sahoo P K & Das R, *J Appl Phys*, 132 (2022) 243101.
13 Surbhi K & Das R, *Photonic Networks and Devices,* (pp. JW3A-39). Optica Publishing Group, (2022, July).
14 Surbhi K & Das R, In *Laser Science* (pp. JW4A-88). Optica Publishing Group, (2022, October).
15 Bikorimana S, Lama P, Walser A, Dorsinville R, Anghel S, Mitioglu A & Kulyuk L, *Opt Express*, 24 (2016) 20685.
16 Dong N, Li Y, Zhang S, McEvoy N, Zhang X, Cui Y & Wang J, *Opt Lett*, 41 (2016) 3936.
17 Wang K, Feng Y, Chang C, Zhan J, Wang C, Zhao Q & Wang J, *Nanoscale*, 6 (2014) 10530.
18 Zhou K G, Zhao M, Chang M J, Wang Q, Wu X Z, Song Y & Zhang H L, *Small*, 11 (2015) 694.
19 Surbhi K, Bhakta S, Sahoo P K & Das R, *J Appl Phys*, 132 (2022) 243101.